Journal of Ovonic Research Vol. 11, No. 1, January - February 2015, p. 27 - 34

CHARACTERIZATION OF PHOSPHORUS-DOPING IN ZINC OXIDE PELLETS USING SOLID STATE REACTION METHOD

F. MALIK[a], M. ASGHAR[a*], K. MAHMOOD[b], M.Y.A.RAJA[c], A. NAWAZ[a], R. TSU[c], M. F. WARSI[a]

[a] *The Islamia University of Bahawalpur-63100, Pakistan*
[b] *G. C. University Faisalabad-68000, Pakistan*
[c] *UNC-Charlotte, NC-28326 USA*

A drop of phosphorus 'spin on dopant 430' was sprayed on ZnO pellets (prepared from 99.999% ZnO powder) and sintered in air in the temperature range of 500 to 1000°C with a step of 100°C for one hour in a programmable diffusion furnace. Characterization of as-prepared ZnO pellets was performed by various diagnostic techniques: e.g., X-ray diffraction confirmed hexagonal structure of ZnO pellets preferably along (002) direction. We observed forward shift in 2 theta value of the X-ray diffraction pattern of ZnO sintered at temperature 1000°C. We correlate the forward shift with the involvement of phosphorus with vacancy at Zn site. Theoretical calculations on a 32-atoms super cell of phosphorus doped ZnO further supported the argument in the shape of a shallow acceptor P_{Zn} - $2V_{Zn}$ complex on Zn site. Typical PL spectra displayed band-to-band transitions peak and an additional donor-acceptor peak at ~3.14 eV in all samples.

(Received December 7, 2014; Accepted January 16, 2015)

Keywords: Zinc Oxide, Photoluminescence, X-ray Diffraction.

1. Introduction

Zinc oxide is a well-known II/VI semiconductor with potential applications in optoelectronic devices due to its direct wideband gap and large exciton binding energy [1, 2]. But the greatest challenge for these applications, however, remains with the fabrication of reliable and stable p-type ZnO with low resistivity and high carrier concentration [3]. This p-type doping issue is related with the formation and compensation effects of native donor defects such as oxygen vacancies (V_O) and zinc interstitials (Zn_i) higher activation energy of acceptors in the band gap of ZnO [4-6]. We find in literature that even though nitrogen and phosphorous are the most favorable p-type dopants in ZnO, but stable p-type conductivity is hard to achieve due to their low solubility [7]. Table I enlists detail of various acceptors reported in ZnO [8-13].

---

[*] Corresponding author: mhashmi@iub.edu.pk

Table I Literature review on p-type conductivity of ZnO.

Type	Methods	Characterization Techniques	Annealing Temperature	Comments	References
p-type ZnO	RF Sputtering	XRD, Hall, SIMS, TEM	200 to 300 °C	Doping of P in ZnO is used to minimize the oxygen vacancy and zinc interstitial. They purposed a self-compensation mechanism which may increase the accepter impurities to make ZnO p-type.	8
p-type ZnO	Pulsed laser deposition	Resistivity, SEM, PL	1000 °C for 12 hour	By reducing the shallow donors, to achieve p-type ZnO	9
p-type ZnO	Physical vapor transport technique without any catalysts	EDAX, Rutherford backscattering spectrometer, XRD, PL, HRTEM		Phosphorus is substitute to oxygen.	10
p-type ZnO	RF Sputtering	XRD, Hall, PL, UV spectrometer, IV measurements	Rapid thermal annealing at 800 °C for 5 min	P occupies Zn site and combines with two Zn vacancies to form P_{Zn}–$2V_{Zn}$ accepter complex. Shallow accepter is responsible for p-type conductivity.	11
p-type ZnO	RF Sputtering	XRD, Hall, PL	400 to 550°C	p-type conductivity is activated by post annealing.	12
p-type ZnO	RF Sputtering	XPS, SIMS, XRD		O^{-2} anions were substituted by P^{-3} anions and responsible for p-type conductivity and also increasing the concentration of P in ZnO, forming the P-related accepter	13
p-type ZnO	Solid Sate Reaction	XRD, PL, SEM, Hall Probe	500-1000 °C	i. Phosphorus replaces Zn site and comparatively smaller size of P allows Zn vacancies to form P_{Zn}–$2V_{Zn}$ accepter complex. ii. Phosphorus occupies oxygen site forms deeper accepter.	This study

The diffusion limit for acceptor impurities in ZnO, as well as other wide bandgap materials suffering from doping asymmetry, can be enhanced above the thermodynamic limit by employing “non-equilibrium” conditions. One of the ways to improve the dopant diffusion is by adjusting its chemical potential: μA, a determinant of the dopant solubility in the material [14]. Larger potential value would increase the site occupation by the dopant in lattice and preclude precipitation, as well. High temperature sintering is yet another way to facilitate the enhancement of acceptor/donor concentration in ZnO. High temperature sintering can generate the acceptor/donor ions in ZnO. For example, it may support the formation of P_O (phosphorus on oxygen site) and/or (P_{Zn}, V) defects in ZnO lattice [15]. Therefore, high temperature sintering study is understood as very helpful technique to fabricate somewhat stable p-type ZnO.

We report in this paper, a systematic preparation of phosphorous doped bulk ZnO by solid state reaction method. The ZnO pellets were sintered from 500 to 1000 ^oC in a programmable diffusion furnace. X-ray diffraction pattern associated with the sintered samples exhibited forward shift in ‘2 theta’ values of the signature peaks. Theoretical calculations regarding 32-atoms super cell of ZnO revealed that the involvement of P on Zn and/or O sites resulted in appearance of shallow acceptor ($P_{Zn} - 2V_{Zn}$) and/or deep acceptor level (P_O), respectively. The results were further supported with the help of PL, Hall probe and SEM measurements. In rest of the paper, experimental summary, results and discussions, and concluding remarks are arranged as sections 2, 3 and 4, respectively.

2. Experimental Summary

The ZnO powder with purity 99.99% was purchased from Aldrich ™, was used as starting material for the fabrication of pellets ZnO powder with purity 99.99%. The hydraulic press with high pressure of 5 ton was used for the preparation of pellets. A drop of phosphorus ‘spin on dopant 430’ was sprayed on the surface of pellets and which then underwent to sintering process. The pellets were sintered at different temperatures from 500 to 1000^oC, keeping a step of 100^oC using a programmable diffusion furnace for an hour. The characterization of sintered samples of ZnO was performed using following equipments; SEM (3000 Hitachi), PL/Raman (Photon Systems) having laser wavelength 248 nm, Ecopia 3000 for Hall Measurement and XRD (Miniflex Rigaku). All the measurements were performed at room temperature.

3. Results and Discussion

The systematic and careful characterization was performed using the apparatus and equipment listed in section 2. Figure 1 displays the SEM images of P-doped ZnO pellets sintered at different temperatures from 700 to 1000 ^oC with a step of 100 ^oC as noted earlier. It is evident from figure 1 that the average crystallite size increases with the sintering temperature. Such observation could be understood or reconciled as the promotion of the nucleation process leading to the increase of crystallinity in the pallets.

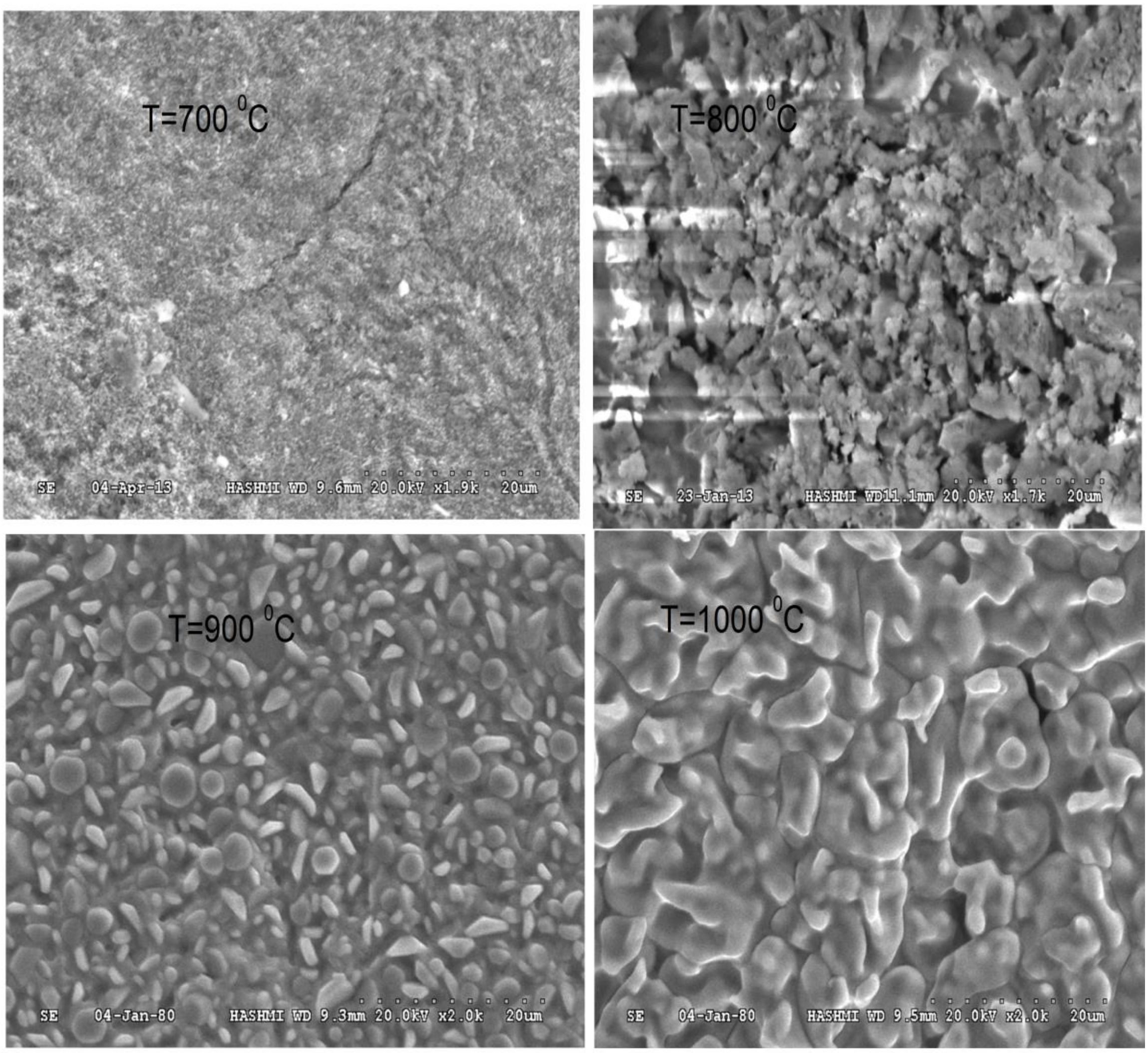

Fig. 1: SEM images of P-doped ZnO pellets annealed at different temperature. Crystallinity of the pellet improves with increasing annealing temperature.

Typical XRD patterns of the P-doped ZnO pellets sintered at the different temperature (500^{o}C to 1000 ^{o}C with a step of 100 ^{o}C) for one hour demonstrated shift in ‘2 theta values’ of 8 diffraction peaks corresponding to the ZnO (1 0 0), (0 0 2), (1 0 1), (1 0 2), (1 1 0), (1 0 3), (2 0 0) and (1 1 2) planes, respectively. Comparison with JCPD 36-1451 Card confirmed the formation of hexagonal zinc oxide [11, 12, and 16]. For clarity, we have displayed only the dominant diffraction peaks corresponding to (0 0 2) plane, in Figure 2.

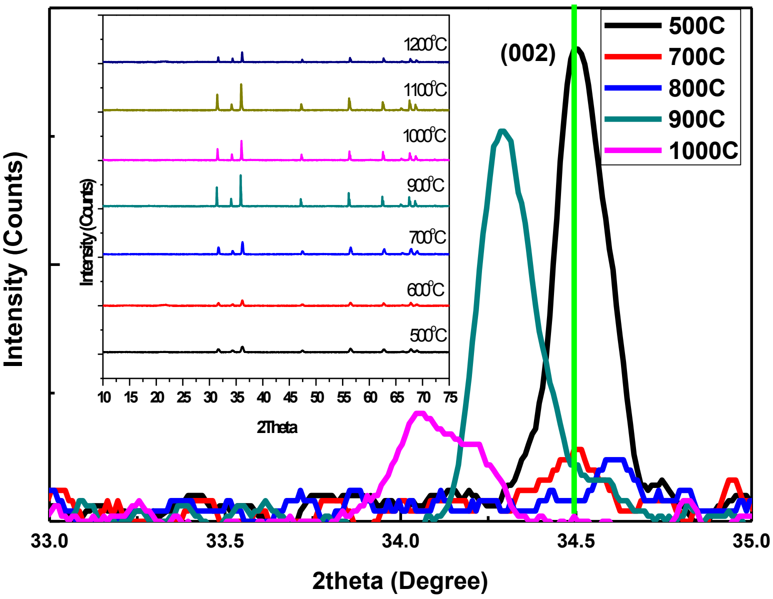

Fig. 2: X-Ray Diffraction pattern of P-doped bulk ZnO annealed at 600^{o}C -1000 ^{0}C shows that (0 0 2) plane of ZnO shifts towards higher 2theta values with sintering temperature. Inset of figure 2 demonstrated XRD pattern of un-doped pellets.

We clearly see that 2θ value of the major peak of the representative ZnO samples varies with the sintering temperature. The 2θ value of the peak increases and reaches 34.6^{o} at T_{sinter} = 800^{o}C. The inset of figure 2 demonstrates the XRD pattern of un-doped samples and annealed at different temperatures. It is clear from figure that peak position of (002) plane for un-doped ZnO is fixed at 34.5^{0}, but the shifting of peak only observed in P-doped samples. Owing to Bragg's equation ($n\lambda = 2d \sin\theta$, d is lattice constant), the forward shift in 2θ value is related with decrease of lattice constant of the crystal. Now considering the atomic size of P, an increase in lattice constant is expected when P atom occupies O site (smaller in size than P); on the other hand, the lattice constant decreases when P atom occupies Zn site (larger in size than P) [17]. Practically, the (0 0 2) plane of the ZnO shifts towards higher 2θ value with the sintering temperatures up to 1000^{o}C and thus yields smaller lattice constant. Hereafter, we will refer the filling of Zn site and the O-site filled with P atoms as A-type shift and B-type shift, respectively. In order to confirm the foresaid argument, using Quantum ESPRESSO software package, we simulated the 32 atoms super cell of ZnO by replacing Zn with P atom and O with P. Consistent with the earlier option, the replacement of P with Zn hereby, was possible only by reducing lattice constant ~ 7% and as result the lattice relaxed at the cost of two Zn vacancies in the super cell. The detail can be seen in figure 3; where P has replaced Zn atom in row 3 (from top) and as a result, two Zn atoms are missing in row 2 and 3. Accordingly, the information from the literature support our calculations that a P atom while occupying Zn site may generate two Zn vacancies and hence produces a shallow acceptor P_{Zn}–$2V_{Zn}$ complex above the valence band maxima (response can be seen in the diagram of ZnO, on right side of figure 3). In this way, the A-type shift of (0 0 2) plane leads to p-type conductivity of ZnO. Hall measurements of the samples strengthened the interpretation of the observation and yielding free hole concentration as $(4.35 \pm 0.25)\times 10^{15}$ cm^{-3}.

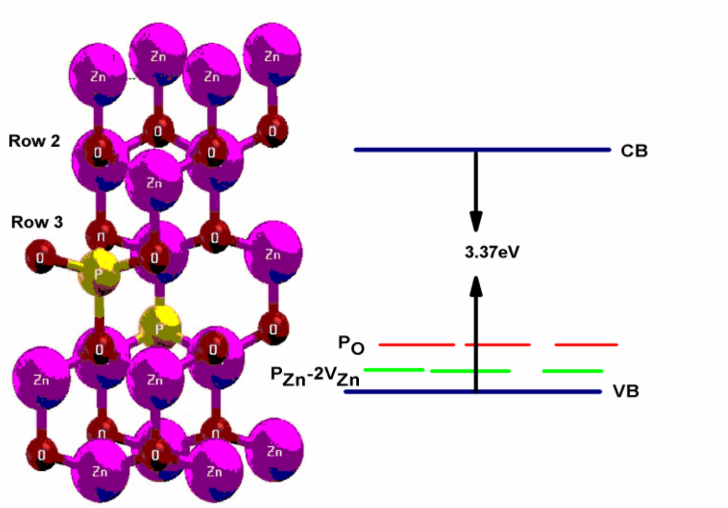

Fig. 3. (left) Simulation results of 32 atoms super cell of ZnO doped with P atoms. The PZn - 2VZn complex is evident in combination of row 2 and 3 of the cell, (right) shallow and deep acceptor levels associated with PZn - 2VZn complex and PO, respectively.

Furthermore, two possible mechanisms of p-type ZnO by doping of phosphorus (P) have been discussed in literature. (a) If phosphorus replaces oxygen to form P_O; it will act as an acceptor [19, 20]. Theoretical calculations suggest, an acceptor P_O could be formed at energy level of 0.49 eV above the VBM which is a deep accepter [21] and hence cannot contribute to p-type conductivity in ZnO; (b) on the other hand, if P replaces Zn atom; owing to its size, it would generate two vacancies at Zn sites additionally, to form a complex ($P_{Zn} – 2V_{Zn}$) complex [22, 23]. The ($P_{Zn} – 2V_{Zn}$) complex acts as an acceptor level. X. H. Pan et al, experimentally worked out the activation energy of the ($P_{Zn} – 2V_{Zn}$) complex and found it in the range of 0.127-0.180 eV which is obviously much smaller than that of P_O defect i.e.0.49 eV above the VBM [24]. The calculations, therefore are in agreement with our simulation results on ZnO super cell. To support the observation, we performed further measurements described in the following:

The room temperature PL (photoluminescence) measurements were carried out to examine the effect of sintering on the optical properties of the P-doped ZnO pellet. Figure 4 demonstrates typical PL spectra of the doped samples measured at room temperature.

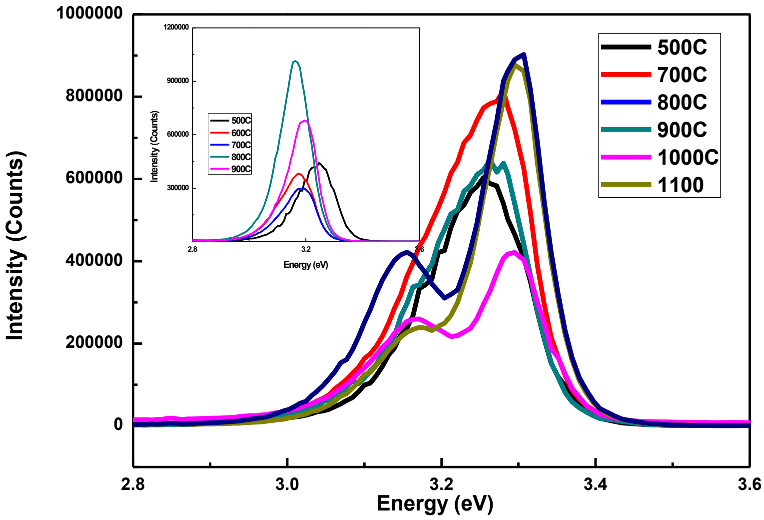

Fig. 4: Photoluminescence spectra of P-dopped ZnO powder annealed at 500oC -1100oC. Additional peak at around 3.14 eV in doped pellets is associated with PZn – 2VZn complex. For comparison inset of this figure showed the PL spectra of un-doped ZnO pellet

All samples exhibit band to band emission at 3.31 eV and in addition, an additional peak at 3.15 eV also appears [25]. This additional peak is related with donor-acceptor pair i.e. $P_{Zn} – 2V_{Zn}$ complex. The inset of figure 4 depicts PL data of un-doped samples annealed at different temperatures. This figure shows that all samples consist of only band to band emission peak and there is no donor acceptor pair peak. Presence of the additional peak in doped ZnO sample clearly supports acceptor-donor defect therein. The binding energy of P-doped ZnO pellets can be evaluated using the relation [26]

$$E_A = E_{gap} - E_{FA} + k_B T/2 \qquad (1)$$

E_{gap} is bandgap of ZnO and E_{FA} transition energy level. The measured E_A value was found to be 160 meV, consistent with the already reported values for $P_{Zn} – 2V_{Zn}$ complex [9]. The absence of donor acceptor in un-doped ZnO pellets strongly suggested that P atom diffuses into ZnO at sintered temperature 1000 °C and form complexes with two zinc vacancies.

4. Conclusions

In conclusion, we have successfully enhanced the phosphorous diffusion in ZnO pellets to achieved p-type conductivity. ZnO pellets were doped with P using high temperature sintering conditions. The diffusion of P atoms in ZnO increases with sintering temperature. The shifting of X-ray diffraction peaks of ZnO plane towards higher ‘2-theta’ angle and emerging of donor acceptor pair excitation in PL spectra strongly suggested that the diffusion of P atoms is temperature dependent. Results were supported by simulation of 32 atoms super cell of ZnO as well.

Acknowledgements

Authors are thankful to Higher Education Commission Pakistan for financial support under project No. 2913/R&D and Northrop Grumman Corp for the financial support. The authors are also thankful to department of Physics and Optical Sciences and Cameron Research Center UNC-Charlotte, USA for technical support.

References

[1] M. Asghar, K. Mahmood , R. Tsu, Y-H. Xie, M-Y-A. Raja, I-T. Ferguson, Semi. Conduct. Sci. Technol. **28,** 105019 (2013).
[2] M. Asghar, K. Mahmood, M-A Hasan, Key Eng. Mater. **510,** 132 (2012).
[3] J. M. Qin, B. Yao, Y. Yan, J. Y. Zhang, X. P. Jia, Z. Z. Zhang, B. H. Li, C. X. Shan, D. Z. Shen, Appl. Phys. Lett. **95**, 022101 (2009).
[4] D. Sentosa, Liu B, L.M. Wong, Y.V. Lim, T.I. Wong, Y.L. Foo, H.D. Sun, S.J. Wang, Thin Solid Films **520**, 994 (2011).
[5] O. Min-Suk, H. Dae-Kue, C. Yong-Seok, K. Jang-Won, P. Seong-Ju, H. Chi-Sun, C. Kyoung Ik, Appl. Phys. Lett. **93**111905 (2008).
[6] L. J. Mandalapu, F. X. Xiu, Z. Yang, D. T. Zhao, J. L. Liu, Appl. Phys. Lett. **88,** 112108 (2006).
[7] J. Bian, X. Li, C. Zhang, L. Chen, Q. Yao, Appl. Phys. Lett. **84,** 3783 (2004).
[8] H. Guangxia, G. Hao, Acta Materialia. **56,**5066 (2008).
[9] C. X. Shan, Z. Liu, S.K. Hark, Appl. Phys. Lett. **92**, 073103 (2008).
[10] J J. Karamdel, C.F. Deeb, K.G. Saw, B. Varghese, C.H. Sow, I. Ahmad, B.Y. Majlis, J. Alloy. Compnd. **512**, 68 (2012).
[11] S.C. Su, X.D. Yang, C.D. Hu, Physica B **406,** 1533 (2011).

[12] D. Ruiqin, Z. Huiqun, W. Yi, Mater. Lett. **62**, 498 (2008).
[13] H. Guangxia, G. Hao, W. Yu, H.F. Liu, J. Apply. Phys. **106**, 123522 (2009).
[14] S.H. Wei, Computational Mater. Sci. **30,** 337 (2004) .
[15] H. Von Wenckstern, G. Benndorf, S. Heitch, J. Sann, M. Brandt, H. Schimdt, J. Lenzner, M. Lorenz, A.Y. Kuznetsov, B.K. Meyer, M. Grundmann, Appl. Phys. A **88,** 125 (2007).
[16] V. Vaithianathan, K. Asokan, P. Jae Young, Appl. Phys. A **94**, 995 (2009).
[17] K.S. Navendu G, Dhirendra, Phys E **42,** 1675 (2010).
[18] Z.G. Yu, H. Gong, P. Wu, Chem. Mater. **17**, 852 (2005).
[19] H. Dae-Kue, O. Min-Suk, L. Jae-Hong, K. Chang-Goo, P. Seong-Ju, Appl. Phys. Lett. **90,** 021106 (2007).
[20] A.F. Kohan, G. Ceder, D. Morgan, Phys. Rev. B **61**, 15019 (2007).
[21] L. Woo-Jin, K. Joongoo, K.J. Chang, J. Korean Phys. Soci. **53**, 196 (2008).
[22] Z.G. Yu Z, H. Gong, P. Wu, Appl. Phys. Lett. **86,** 212105 (2005).
[23] G. Li, L. Baoting, L. Qiang, Z. Yang, G. Jianxin, J. Guoqi, Z. Qingxun, W. Yinglong, F. Guangsheng, Physics Letters A **375**, 939 (2011)–945.
[24] X. H. Pan, J. Jiang, Y. J. Zeng, H. P. He, L. Zhu, P, Z. Z. Ye, B. H. Zhao, J. Apply. Phys. **103,** 023708 (2008).
[25] V. Veeramuthu, H. Shunichi, P. Jae Young, K. Sang Sub, J. Appl. Phys. **102**, 086107 (2007).
[26] H. Dongqi Y, Lizhong, Q. Shuangshuang, Z. Heqiu, L. Song-En Andy, L.K. Len, F. Qiang, C. Xi, S. Kaitong, J. Phys. D: Appl. Phys. **42,** 055110 (2009).